REX: GPU-Accelerated Sim2Real Framework with Delay and Dynamics Estimation

Anonymous authors
Paper under double-blind review

Abstract

Sim2real, the transfer of control policies from simulation to the real world, is crucial for efficiently solving robotic tasks without the risks associated with real-world learning. However, discrepancies between simulated and real environments, especially due to unmodeled dynamics and latencies, significantly impact the performance of these transferred policies. In this paper, we address the challenges of sim2real transfer caused by latency and asynchronous dynamics in real-world robotic systems. Our approach involves developing a novel framework, REX (Robotic Environments with jaX), that uses a graph-based simulation model to incorporate latency effects while optimizing for parallelization on accelerator hardware. Our framework simulates the asynchronous, hierarchical nature of real-world systems, while simultaneously estimating system dynamics and delays from real-world data and implementing delay compensation strategies to minimize the sim2real gap. We validate our approach on two real-world systems, demonstrating its effectiveness in improving sim2real performance by accurately modeling both system dynamics and delays. Our results show that the proposed framework supports both accelerated simulation and real-time processing, making it valuable for robot learning.

1 Introduction

Sim2real, the transfer of control policies from simulation to the real world, is crucial in robotics due to its ability to solve tasks efficiently without the risks associated with real-world learning (Rudin et al., 2022; Tan et al., 2018). With recent advancements in physics simulation on accelerator hardware (NVIDIA, 2020; Hu et al., 2020; Freeman et al., 2021; Todorov et al., 2012), parallelized simulations have greatly reduced training times for complex tasks (Rudin et al., 2022; Hoeller et al., 2024). However, discrepancies between simulation and reality, such as unmodeled dynamics, often reduce the effectiveness of these policies in real-world applications. Addressing this 'sim2real' gap is essential for effective transfer of policies from simulation to the real world.

A critical yet often overlooked issue in sim2real transfer is the impact of latency in real-world systems, which can degrade performance (Tan et al., 2018; Ibarz et al., 2021; Elocla et al., 2023; van der Heijden et al., 2024b). The real world is inherently asynchronous, with delayed sensor data causing agents to act on outdated information. Additionally, slow policy evaluations can further delay an agent's actions, compounding these latency issues and leading to suboptimal performance. To mitigate these effects, Fig. 1 illustrates two common compensation strategies: simulating delays during training (Fig. 1c) (Tan et al., 2018; Elocla et al., 2023; van der Heijden et al., 2024a) and using an estimator to predict future states (Fig. 1d) (Smith, 1957; Sherback et al., 2006; Augugliaro et al., 2014; Yang et al., 2020). However, both strategies have limitations. Delay simulation complicates training because the agent's input must include a history of observations and actions to restore the Markov property, while an estimator requires accurately modeled system dynamics and delays, which are often difficult to identify (Unbehauen & Rao, 1990).

The hierarchical and asynchronous nature of robotic systems further complicates accurate and efficient simulation on accelerator hardware. Unlike conventional RL, which assumes a single, synchronized environment (Brockman et al., 2016), robotic systems consist of interconnected models operating at different rates, with

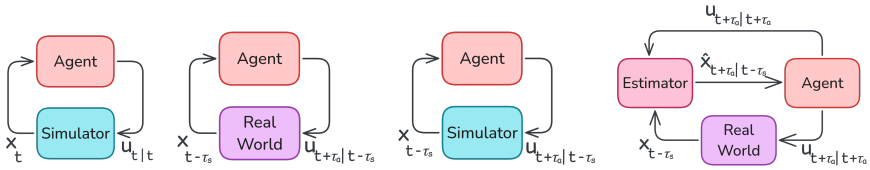

(a) Naiive (b) Real world (c) Delay simulation (d) Delay compensation

Figure 1: A policy trained in simulation (a) may perform suboptimally in the real world (b) due to delays. The notation $u_{t+\tau_a|t-\tau_s}$ denotes that an action u is applied at $t+\tau_a$ based on information up to $t-\tau_s$, where τ_a and τ_s are the actuation and sensing delays, respectively. By simulating these delays during training (c), the sim2real gap with (b) can be reduced. Alternatively, an estimator (d) can predict future states and compensate for delays, improving policy transfer from (a) to (d). The notation $x_{t+\tau_a|t-\tau_s}$ denotes that a state x is predicted at $t+\tau_a$ based on information up to $t-\tau_s$.

asynchronous communication introducing complexities like inter-model latencies and stochastic dynamics (Quigley et al., 2009; Baheti & Gill, 2011), leading to irregular computation patterns. Irregular execution paths require serialization, reducing GPU efficiency, and while simulating time-scale differences improves sim2real accuracy, it further exacerbates this inefficiency (Shibata, 2010).

The main contribution of this paper is a sim2real framework, REX (Robotic Environments with jaX), that introduces a graph-based simulation model with latency effects, optimized for parallelization on accelerator hardware. The framework's innovation lies in its ability to simulate asynchronous, hierarchical systems by explicitly modeling computation, communication, actuation, and sensing delays, while incorporating delay compensation strategies for improved sim2real transfer. Parallelization in both state and parameters allows for simultaneous estimation of system dynamics and delays from real-world data, efficiently minimizing the sim2real gap. Additionally, it supports real-world deployment by distributing computations across CPU cores and accelerators, optimizing for latency and performance.

For RL and robotics practitioners, this framework offers several advantages. It enables modeling of both simulated and real-world systems through a unified, ROS-like graph-based pipeline (Quigley et al., 2009). The framework supports accelerated training speeds familiar to RL workflows and reduces the sim2real gap by refining models with real-world data. Integration with the JAX (Frostig et al., 2018) ecosystem further supports advanced RL training and optimization (Lange, 2022b;a; Tang et al., 2022; Lu et al., 2022).

Building on these advantages, we make four key claims: Our framework (i) enables the identification of both dynamics and delays from real-world data, (ii) implements delay compensation and simulation techniques that are essential for effective sim2real transfer, (iii) facilitates efficient parallelized offline simulation on accelerator hardware, (iv) supports real-time online processing capabilities that meet the latency and performance requirements of real-world systems. These claims are supported by experiments on two real-world systems. The pendulum swing-up task clearly demonstrates how neglecting delay simulation can impair policy transfer, highlighting the need for delay-aware approaches, while the quadrotor task shows scalability to more complex robotic systems. The code and interactive examples are available as supplementary material.

2 Related Work

Sim2Real Frameworks Sim2real frameworks like Orbit (Mittal et al., 2023), Drake (Tedrake & the Drake Development Team, 2019), and EAGERx (van der Heijden et al., 2024b) facilitate the transfer of control policies from simulation to real-world settings. However, they generally do not include direct support for delay or dynamics identification from real-world data. Our framework addresses this gap by integrating these capabilities directly into the framework. Orbit utilizes Nvidia PhysX for parallelized simulations on accelerator hardware (NVIDIA, 2020). Our framework is based on JAX (Frostig et al., 2018) to support parallelized computation on accelerator hardware, while also enabling automatic differentiation. Moreover, our framework, like EAGERx (van der Heijden et al., 2024b), is not restricted to a specific physics engine,

as long as the engine is compatible with JAX, such as Brax (Freeman et al., 2021) or the MJX extension of Mujoco (Todorov et al., 2012). This flexibility enables users to select and extend engines as needed within the graph-based model.

Delay Estimation System identification involves estimating a system's dynamics from input-output data and is a well-established area of research (Ljung, 1998). Traditional methods primarily focus on linear systems, often utilizing least-squares optimization techniques (Van Overschee & De Moor, 2012), while more recent efforts have extended to nonlinear systems (Nelles, 2020). Recent advances leverage the differentiability of general-purpose simulators to estimate complex system dynamics (Le Lidec et al., 2021; Heiden et al., 2022; Caluwaerts et al., 2023). Our approach builds on these advancements by extending simulators with delay dynamics, allowing for the joint estimation of both system dynamics and delays. Instead of gradient-based methods, we use evolutionary strategies (Hansen, 2006), which we found to be less susceptible to local minima and better utilize the parallelism of modern hardware (Tang et al., 2022).

Delay Simulation Frameworks like Drake and EAGERx provide support for fixed delay simulation (Tedrake & the Drake Development Team, 2019; van der Heijden et al., 2024b). Our framework, however, extends this capability by supporting stochastic delay simulation using Gaussian Mixture Models (GMMs). Additionally, it incorporates correlations between delays by considering the system's topology and communication structure during simulation. Although our framework allows for correlated delays, these delays are data-independent and do not change based on the simulated data. For example, even if an object detection algorithm takes longer to process when multiple objects are in view, our simulated delays remain the same regardless of the number of detected objects.

Delay Compensation Delay compensation in sim2real has been addressed through various methods. Algorithmic approaches for compensating delays have been proposed by Schuitema et al. (2010); Bouteiller et al. (2021). Other studies have enhanced sim2real performance by simulating delays during training and using a history of observations and actions as policy inputs (Tan et al., 2018; van der Heijden et al., 2024b). These methods teach policies to handle delays without compensating for them directly during real-world execution. Direct compensation techniques, such as the Smith predictor (Smith, 1957), have long been used in robotics to manage delays from sensors, actuators (Sherback et al., 2006; Augugliaro et al., 2014), and planning latency (Yang et al., 2020). In our work, we demonstrate that by compensating for delays during execution, we can eliminate the need for delay simulation during training, resulting in a more efficient training process while maintaining high performance in real-world applications.

3 Our Sim2Real Framework

In this section, we present a our framework for sim2real transfer in robotics, focusing on accurately modeling and compensating for the asynchronous interactions and delays encountered in real-world systems. In the following, we will first describe the graph-based architecture that facilitates asynchronous message passing and delay modeling. We will then detail the three runtime configurations designed for simulation, accelerated training, and real-time deployment. Finally, we will cover the integration of system identification techniques and delay compensation strategies to bridge the gap between simulation and reality.

3.1 Overview

The central element of our framework is the node, which represents a discrete unit of computation or sensing, operating asynchronously within the system. Nodes are designed to run at specified rates, processing inputs, maintaining state, and generating outputs. In our approach, both real-world and simulated systems are implemented as networks of these nodes, where communication occurs via directed edges, as shown in Fig. 2a. Each node's operation is defined by a step function that determines its behavior, transforming inputs into outputs. For example, nodes can represent various components such as cameras, agents, or motors, each handling specific tasks like sensing, control, or actuation. This modular design allows for flexible state, time, and action abstractions, supporting the modeling of complex interactions in a decentralized manner. Nodes are interconnected in a directed graph, facilitating asynchronous message passing and enabling nodes to

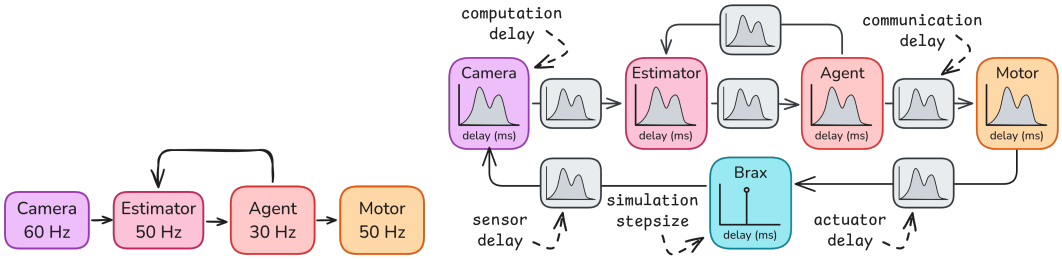

(a) Real-world system

(b) Simulated system with delays

Figure 2: Comparison between a real-world system setup and a simulated system with integrated delays. The real-world system (a) operates with different nodes at specified rates, while the simulated system (b) incorporates various types of delays to closely mimic real-world timing behaviors, including sensor, actuator, communication, and computation delays.

operate at different rates. This design also enables the swapping of real-world nodes with simulated nodes, resulting in a unified software pipeline that can be used for sim2real transfer.

Asynchronous operations is inherent in real-world systems due to network transmission times, processing lags, or mechanical response times, which introduces delays into the system dynamics. To address this, we introduce a delay simulation model that captures both deterministic and stochastic delays, incorporating realistic timing behavior through delay distributions for communication, computation, sensor, and actuator delays. As shown in Fig. 2b, our model explicitly defines these delays as non-negative distributions, ensuring that the timing characteristics of the simulated environment closely match those of the real world. While this provides the structure for delay simulation, the challenge of estimating the correct delay parameters is addressed later in Sec. 3.3.

The framework supports multiple communication protocols to manage the flow of messages between nodes, allowing users to specify whether each communication channel should be blocking or non-blocking. A blocking channel ensures that a receiver node waits for the most recent message before processing, which minimizes latency in real-time systems by avoiding outdated information. However, blocking channels can introduce instability if delays cause unforeseen propagation through the graph; in such cases, non-blocking channels may be preferable. For example, an estimator node might opt for non-blocking behavior to continue predicting the system's state when sensor messages are delayed, allowing the controller to maintain responsive operation.

3.2 Runtimes

Our framework leverages JAX (Frostig et al., 2018) for efficient computation, utilizing its ability to perform just-in-time (JIT) compilation and automatic differentiation, which are crucial for high-performance machine learning applications. Nodes are defined using a generic interface, with parameters, states, and outputs specified using data structures that can be statically analyzed, as shown in Fig. 3a. This approach allows for ahead-of-time (AOT) compilation of the `step` method (Fig. 3a, Line 12) on various architectures, including CPUs and GPUs, thereby reducing latency. By compiling nodes in this manner, they can be seamlessly employed across different runtime modes without modification, ensuring flexibility and efficiency in both real-world and simulated environments. Our framework supports three distinct runtime modes, each tailored for different stages of development, training, and deployment: `WALL_CLOCK`, `SIMULATED`, and `COMPILED`.

The `WALL_CLOCK` runtime is designed for real-time execution on physical hardware, operating at real-time speed with each node's step function running asynchronously at its designated rate (Fig. 3b, lines 1-14). Nodes can be compiled to run on dedicated hardware resources such as separate CPU cores or accelerator hardware, minimizing latency (Fig. 3b, Line 17). After initializing the state of the graph, which aggregates the states of all nodes, the graph can be executed for a specified number of steps while recording the outputs and their corresponding timestamps (Fig. 3b, lines 19-24).

The `SIMULATED` runtime enables faster-than-real-time simulation, allowing for accelerated testing and development without real-time constraints. Message passing is is based on simulated timestamps, that are

```
1  class Agent(Node)
2    def init_params(self, rng, graph_state):
3      return PyTree(a=..., b=...)
4
5    def init_state(self, rng, graph_state):
6      return PyTree(x1=..., x2=...)
7
8    def init_output(self, rng, graph_state):
9      return PyTree(y1=..., y2=...)
10
11   # AOT jit-compile with graph.warmup()
12   def step(self, step_state):
13     ss = step_state  # Shorten name
14     # Read params, and current state
15     params, state = ss.params, ss.state
16     # Current episode, sequence, timestamp
17     eps, seq, ts = ss.eps, ss.seq, ss.ts
18     # Grab the data, and I/O timestamps
19     cam = ss.inputs['cam'] # connectd node
20     cam.data, cam.ts_send, cam.ts_recv
21     # Compute new state, and output
22     new_state = PyTree(x1=..., x2=...)
23     output = PyTree(y1=..., y2=...)
24     # Update step_state for next step call
25     new_ss = ss.replace(state=new_state)
26     return new_ss, output # Sends output
```

(a) Node definition

```
1  # Real-world nodes
2  cam = Camera(rate=60)
3  agent = Agent(rate=30)
4  motor = Motor(rate=50)
5  nodes = [cam, agent, motor]
6  # Connect
7  agent.connect(cam) # Async msging
8  motor.connect(agent, # Last 2 msgs
9                       block=True, window=2)
10 # Runtime: WALL_CLOCK
11 # Used for real-time operation
12 graph = Graph(agent, nodes,
13                  Clock.WALL_CLOCK,
14          RealTimeFactor.REAL_TIME)
15 # Ahead-of-time compilation of
16 # every node's .step() method
17 graph.warmup(devices=...)
18 # Run the graph at agent's rate
19 gs = graph.init() # Graph state
20 for i in range(100):
21   gs = graph.run(gs)
22 graph.stop()  # Halts all nodes
23 # Gather data (outputs, timings)
24 record = graph.get_record()
25 # Convert to data flow
26 df = record.to_graph()
```

(b) Real-world runtime

```
1  # Simulation nodes & connections
2  cam = SimCam(rate=60,      delay=Gauss(0.05, 0.01))
3  agent = Agent(rate=30,     delay=Gauss(0.02, 0.01))
4  motor = SimMotor(rate=50, delay=Gauss(0.04, 0.01))
5  brax = Brax(rate=100,  delay=Deterministic(1/100))
6  nodes = [brax, cam, agent, motor]
7  brax.connect(motor,  delay=Gauss(0.01, 0.01))
8  cam.connect(brax,    delay=Gauss(0.01, 0.01))
9  agent.connect(cam,   delay=Gauss(0.01, 0.01))
10 motor.connect(agent, delay=Gauss(0.01, 0.01),
11                 window=2, block=True)
12 # Runtime: SIMULATED (no throttling)
13 graph = Graph(agent, nodes, Clock.SIMULATED,
14                 RealTimeFactor.FAST_AS_POSSIBLE)
15 graph.warmup(devices=...)  # JIT compilation
16 gs = graph.init() # Graph state
17 for i in range(100):  # Simulates 100 steps
18   gs = graph.run(gs)
19 graph.stop()  # Halts all nodes
20 # Simulated data flow to computation graph
21 cg = graph.get_record().to_graph().augment(nodes)
22 # Runtime: COMPILED (1000 parallel rollouts)
23 graph = CompiledGraph(agent, nodes, cg)
24 rngs = jax.split(jax.random.PRNGKey(0), num=1000)
25 gss = jax.vmap(graph.init)(rngs)  # 1000 states
26 rollout = jax.vmap(graph.rollout)(gss, rngs) # run
```

(c) Simulation runtimes

Figure 3: Examples of runtime configurations, showing different execution modes: `WALL_CLOCK` for real-time operation on physical hardware, `SIMULATED` for accelerated testing without real-time constraints, and `COMPILED` for parallelized execution on accelerator hardware. Node definitions use generic PyTrees that allow for compilation across different architectures for reduced latency. Variable names and notation were slightly shortened for clarity and space.

generated based on the communication protocol of every connection (blocking or non-blocking) and specified delay distributions, replicating real-world asynchronous effects (Fig. 3c, lines 1-14).

The `COMPILED` runtime further leverages accelerator hardware like GPUs or TPUs for parallelized execution by enabling the compilation of entire computation graphs into a single function. This makes this runtime suitable for tasks such as training RL policies and large-scale system identification that can leverage massive parallelism. Data flows from other runtimes (e.g., (Fig. 3b, Line 26)) are converted into a computation graph (Fig. 3c, Line 21) and compiled for parallel execution (Fig. 3c, lines 22-26), encoding the asynchronous effects of real-world interaction or simulated delays and enabling parallel execution on accelerator hardware. By supporting these three runtime modes, our framework provides comprehensive flexibility for a wide range of applications, from real-time deployment to parallelized system identification and policy training.

3.3 System Identification

System identification is crucial for minimizing the sim2real gap by ensuring that the simulated model closely mirrors the real-world system. Our framework facilitates this by identifying both the dynamics and delays inherent in real-world systems, allowing for more accurate simulation and effective delay compensation. In the following, we detail how to build and optimize a tailored computation graph from the real-world data collected to estimate system dynamics and delays (see Fig. 4). Data is collected from the real-world system using the `WALL_CLOCK` runtime, logging not only sensor and actuator data but also the timing information associated with message exchanges between nodes. This includes the timestamps for when a message is received, when a node begins processing, and when it sends out the output. Using this data, we construct a data flow graph that captures node interactions, including the precise timing of messages (see Fig. 4a, and Line 21 in Fig. 3c).

Dynamics The data flow graph serves as a foundation for identifying the system's dynamics. One advantage of using a data flow graph is that it inherently represents asynchronous interactions and correctly encodes time-scale differences between nodes. Accounting for these asynchronous effects is essential, as they can significantly impact the identified system dynamics (Unbehauen & Rao, 1990). Given the data flow graph, our framework builds a tailored computation graph as follows. We augment the data flow graph with a simulator that models the system dynamics by adding simulators nodes at the desired simulation rate. Edges between simulation nodes and real-world-interacting nodes are introduced to pass the simulation state

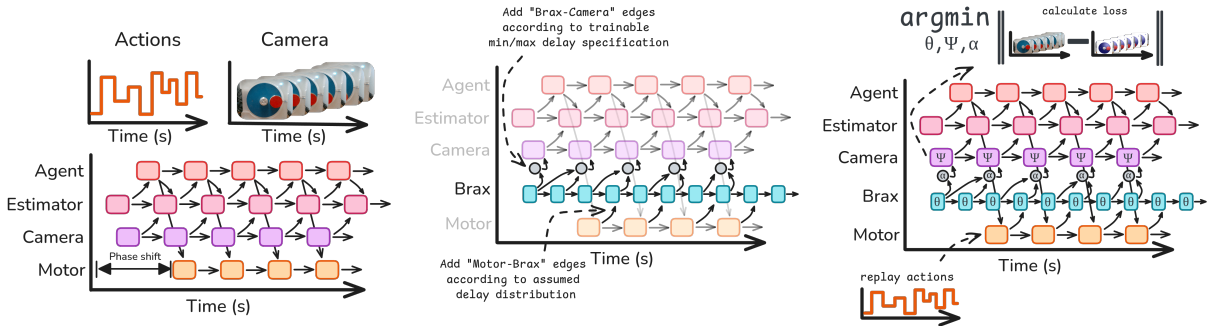

(a) Collected data and data flow (b) Computation graph (c) Optimize

Figure 4: System identification example applied to the system in Fig. 2a. (a) Data collection from the real-world system, including sensor data and timing information. (b) Construction of a computation graph that integrates the data flow with simulated nodes for dynamics and hidden delay identification. Motor-Brax edges are added based on a specified delay distribution, while Brax-camera edges follow a trainable min-max delay specification. (c) Optimization of simulation parameters and delays to minimize discrepancies between simulated and real-world behaviors, focusing on the delay interpolation parameter α and the parameters ψ, θ for the camera and Brax nodes.

to the nodes that model real-world interactions (actuators, sensors, etc.), according to assumed delay distributions, as shown in Fig. 4b. These delay distributions are either trainable or prespecified, as explained later in this section. By replaying actions through the computation graph and comparing the reconstructed outputs with the collected data, we optimize the simulator parameters to minimize a reconstruction loss. During this process, all parameters within the computation graph (e.g. simulator parameters or those in any other nodes), can be optimized. For instance, in the example shown in Fig. 4c, we simultaneously identify Brax's system parameters and the camera's parameters for angle-to-pixel conversion, but we could have also optimize for any other parameter in the graph, such as the motor's friction. The `COMPILED` runtime is particularly advantageous for this optimization process due to its ability to parallelize computations efficiently. We found evolutionary strategies effective for this task, as they leverage parallelism, constraint specification, and are less susceptible to local minima (Hansen, 2006; Tang et al., 2022; Lange, 2022a).

Measurable Delays In addition to dynamics, our framework addresses delay estimation, distinguishing between directly measurable delays and hidden delays, such as those in actuators and sensors. Using the recorded timing data, we estimate the communication and computation delays of the system by fitting a Gaussian Mixture Model (GMM) to the measurable delay data using gradient descent to maximize the likelihood of the data. When sampling from the GMM, we clip the sampled values to be non-negative, as delays are inherently non-negative.

Hidden Delays With hidden delays we mean delays that are not directly observable in the data flow graph, such as delays between the real-world and sensors or actuators. While we support the addition of edges between simulator and real-world-interacting nodes based on prespecified delay distributions (e.g., motor-Brax connections in Fig. 4b), users can also introduce trainable delays to identify hidden delays (e.g., Brax-camera connections in Fig. 4b). Our approach requires specifying a minimum and maximum bound for each trainable delay, which we use to introduce additional edges that accommodate all possible communication patterns between two nodes under minimum and maximum delay conditions. We then introduce a trainable parameter $\alpha \in [0, 1]$ for each connection, allowing interpolation between the minimum and maximum scenarios. Different deterministic interpolation schemes, such as linear or zero-order hold, are currently supported to model various delay characteristics.

3.4 Delay Compensation

Once the system dynamics and delays are identified, the framework supports various strategies for delay compensation to enhance sim2real performance.

Delay Simulation One straightforward strategy is to integrate the identified delay distributions into the simulation environment. This approach, referred to as delay simulation (Fig. 1c), allows the agent to learn policies that are delay aware. Notice that delays make the problem non-Markovian. To address this, a history of observations and actions can be stacked and used as input to the policy to restore the Markov property. This does make the learning problem more challenging, as the agent must learn to solve the task and handle delays simultaneously, as we will show in our experiments.

Estimator While RL approaches often treat the environment as a black box, in sim2real scenarios, we can utilize the identified system dynamics and delays to design a model-based delay compensator that predicts the system's behavior during real-world execution. Inspired by a Smith Predictor (Smith, 1957) and shown in Fig. 1d, our strategy is to predict the state we expect when the corresponding command based on this state reaches the system. By knowing all delays, we can predict when a command will arrive and estimate the system state at that future time. Specifically, when a sensor captures an observation, we timestamp it and subtract the identified hidden delay τ_s to estimate the timestamp of the world's state the observation corresponds to, $t_s - \tau_s$. When the estimator processes the observation at t_e, it can determine when the resulting command will reach the system by adding the expected estimator-to-actuator latency, τ_a, resulting in $t_e + \tau_a$. Thus, the estimator first updates the state up to $t_s - \tau_s$ and then predicts it forward to $t_e + \tau_a$ using the past control inputs and their estimated timestamps. We recommend using an Unscented Kalman Filter (UKF) for this task because it effectively handles non-differentiable and non-linear dynamics, while requiring only a small number of particles that can be efficiently evaluated in parallel (Julier & Uhlmann, 2004). Additionally, in partially observable settings, a UKF can infer the hidden state of the system from observations and provide this state to the agent, enabling training in a fully observable, delay-free environment, which generally facilitates easier learning. In our experiments, we will evaluate the benefits of using such an estimator for delay compensation and compare the performance gains of delay compensation alone versus delay compensation with hidden state estimation.

3.5 Limitations

Our framework does not support running nodes on different machines; computations are restricted to different devices via JAX. This limits the ability to compile nodes for low-level controllers onboard a robot. Additionally, JAX's Just-In-Time (JIT) compilation can lead to long compilation times, although recent updates with function caching have mitigated this to some extent.

The framework estimates hidden delays as deterministic, which is a reasonable assumption for many robotics applications. Nevertheless, stochastic delays can be modeled by adding variability to the deterministically identified delays, for example, to simulate jitter in sensor readings. Furthermore, our delay simulation is state-independent, meaning that while it accounts for the correlation and stochastic nature of delays, it does not adapt to the specific conditions or data of each simulation step. For instance, if an algorithm takes longer to process when there are multiple simulated objects in view, our approach would not capture this increase in processing time that would occur in a real-world scenario.

Finally, simulating stochastic delays on accelerator hardware remains challenging due to the branching they introduce in the computation graph. We rely on a sampling-based approach in (van der Heijden et al., 2024a) to approximate stochastic delays with a fixed number of observed data flows from recorded episodes when parallelizing simulations with the `COMPILED` runtime. By using a large enough number of recorded data flows, we can effectively capture the stochastic behavior of delays while maintaining efficient parallelization.

4 Experimental Evaluation

The main focus of this work is a sim2real framework that addresses asynchronous interactions in real-world systems by modeling delays and using real-world data for accurate system identification and reinforcement learning training. Our experiments are designed to validate the key claims made in Sec. 1 as follows. First, we identify the system dynamics and delays from real-world data, followed by a sim2real transfer evaluation using the identified system while using delay compensation techniques. We validate our approach on two distinct real-world systems: a pendulum swing-up and a quadrotor control task.

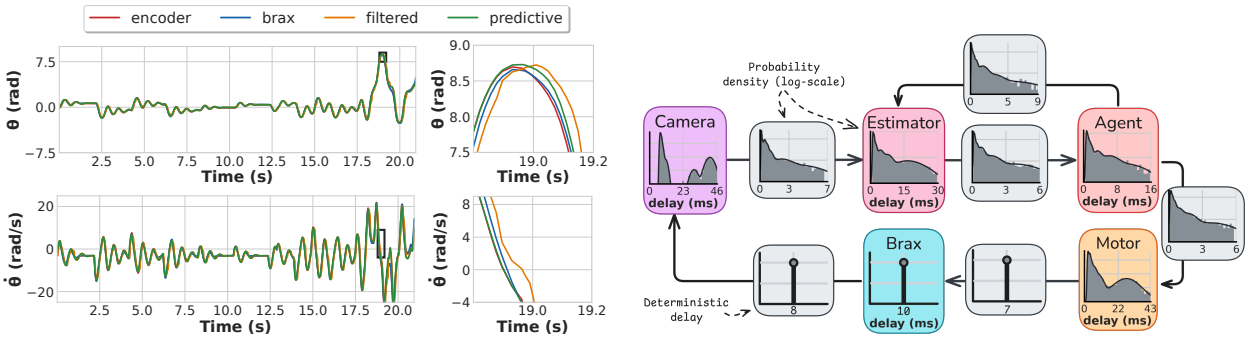

(a) Reconstruction (b) Zoomed (c) Estimated delays

Figure 5: Pendulum system identification and delay estimation. (a) Open-loop reconstruction of the angle (θ) and angular velocity ($\dot{\theta}$) with the *brax* simulator, compared to ground-truth *encoder* data. (b) A zoomed view shows that the *predictive* UKF estimate that compensates for delays, outperforms the *filtered* estimate that does not. (c) Estimated GMM delay distributions and deterministic hidden delays for the camera and motor, with the grey area indicating the measured delay distribution and the black line showing the GMM fit.

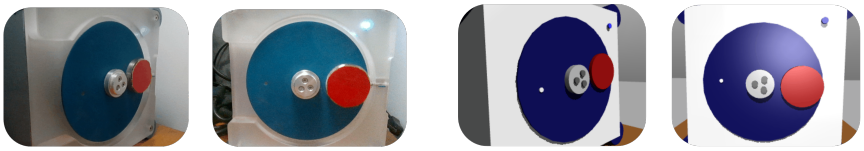

(a) Real images (b) Rendered images with Brax

Figure 6: Comparison of real and rendered images of the pendulum from two different viewpoints. (a) shows actual images captured from side and frontal views. (b) shows the corresponding rendered images from the estimated poses.

	MSE_θ	$\text{MSE}_{\dot{\theta}}$
filtered	0.069	4.256
predictive	**0.012**	**1.114**

Table 1: Mean squared error (MSE) with respect to ground-truth encoder data. Boldface indicates the best performance.

4.1 System Identification and Delay Estimation

To support the claim that our approach enables the identification of both dynamics and delays from real-world data, we present system identification and delay estimation results for the two selected systems.

Pendulum In contrast to the classic swing-up task (Brockman et al., 2016), which uses full state information, our setup relies solely on camera images of the pendulum. This task highlights the challenge of delay estimation and system identification from images. We apply an open-loop voltage sequence to the motor for 21 seconds while recording a stream of images from a RealSense d435i camera, in addition to the applied actions and corresponding timing information. Using this data, we construct a data flow graph that is augmented to form a computation graph, incorporating simulator nodes operating at 100 Hz. We introduce edges between the simulator nodes and the camera and motor via two trainable delays that assume a minimum and maximum delay of 0 to 50 ms, respectively. Images are first preprocessed through background subtraction and color thresholding to detect the center pixel coordinates of the red dot that marks the pendulum's mass. The actions are then reapplied to the simulator, and we optimize the parameters to minimize the reconstruction error between predicted and actual pixel coordinates. Simultaneous optimization is performed on several parameters: the physics parameters of the Brax simulator (mass, length, friction, inertia, etc.), interpolation parameters for hidden camera and motor delays, and the parameters of an ellipse model (center, axes, rotation) that maps pixel coordinates to angles using the intuition that the pendulum's motion (as pixel coordinates) will be an ellipse when projected onto the camera plane. A lightweight dynamics model (Derner et al., 2020) is used in a UKF for full state estimation and delay compensation. We use the Covariance Matrix Adaptation Evolution Strategy (CMA-ES) (Hansen, 2006) to optimize the 27 parameters. Finally, we fit GMMs to estimate delay distributions for all measurable communication and computation delays.

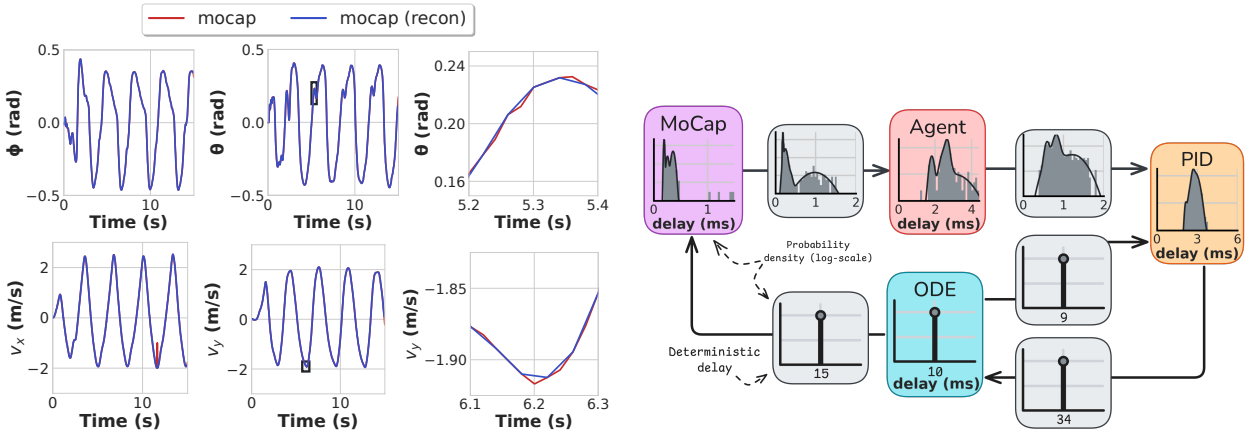

(a) Reconstruction (b) Zoomed (c) Estimated delays

Figure 7: System identification and delay estimation for quadrotor control. (a) Open-loop reconstruction of roll, pitch, and velocities in body frame over 15 seconds (*recon*), showing the accuracy of the identified model compared to the MoCap data (*mocap*). (b) Zoomed view illustrates an accurate fit. (c) Estimated GMM delay distributions, with the grey area indicating the measured delay distribution and the black line showing the GMM fit.

The reconstructed angle and angular velocity from the simulator and estimator are shown in Fig. 5a, alongside the validation data obtained from the pendulum's encoder, which can be considered the ground truth with minimal delay. The open-loop reconstruction remains accurate over a 21-second time horizon. The identified delay distributions are illustrated in Fig. 5c, with a motor-to-Brax delay of approximately 7 ms and a Brax-to-camera delay of around 8 ms. The camera delay exhibits a multi-modal distribution, suggesting variability due to internal processing and shutter speed. The effectiveness of delay compensation is demonstrated in Fig. 5b by comparing the filtered and predictive estimates. The filtered estimate shows the UKF's state estimate plotted against the timestamp of when the action using the estimated state was applied to the simulator, resulting in a noticeable phase shift of around 50 ms. In contrast, the predictive estimate forecasts the filtered estimate forward, resulting in a lower mean squared error (MSE) for both the angle and angular velocity, as shown in Tab. 1. Finally, we use the identified system to render images from the estimated poses, as shown in Fig. 6. The comparison between real and rendered images from two different viewpoints qualitatively demonstrates the accuracy of the estimated system parameters.

Quadrotor Next, we identify the dynamics and delays of a quadrotor system using real-world data to demonstrate the applicability of our approach to higher-dimensional state-action spaces. The quadrotor's yaw is fixed, while reference roll and pitch angles and a height setpoint are sent to a PID controller to maintain a circular flight path at a constant altitude. The PID controller converts the height setpoint to a thrust command, which, along with the roll and pitch commands, is sent to the Crazyflie. We record the actions, timing data, and state information captured by a motion capture (MoCap) system. Similar to the pendulum experiment, we construct a data flow graph that is augmented to form a computation graph with simulator nodes operating at 100 Hz. Edges are introduced between the simulator nodes and the MoCap and PID nodes, incorporating hidden delay nodes with a minimum and maximum delay of 0 to 50 ms, respectively. A dynamics model similar to that used in Kooi & Babuska (2021) is employed. Simultaneous optimization is performed on dynamics parameters (e.g., mass, drag, motor characteristics), interpolation parameters for hidden delays between the dynamics model, MoCap, and PID controller, using CMA-ES (Hansen, 2006) to optimize the 8 parameters. We also fit GMMs to estimate delay distributions for all measurable communication and computation delays.

The results in Fig. 7a show accurate reconstruction of the quadrotor's states over 15 seconds. Identified delays are shown in Fig. 7c, with PID-to-ODE delay at 34 ms, ODE-to-PID delay at 9 ms, and ODE-to-MoCap delay at 15 ms. In the next section, we evaluate the advantage of delay-aware system identification for sim2real transfer, by training policies with and without considering delays.

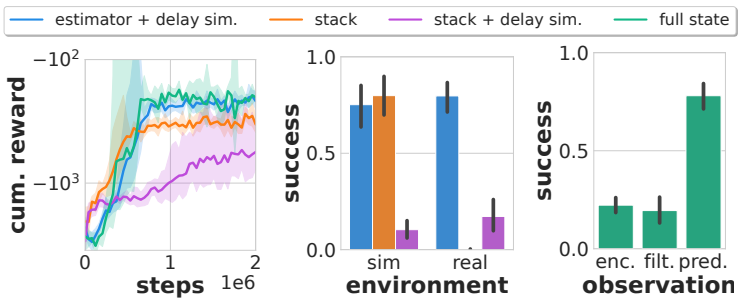

(a) Training curve (b) Sim2real (c) Estimator

Figure 8: Sim2real evaluation of policies trained under different delay and observation conditions for the pendulum swing-up task. (a) Training curves comparing policies with full state information and stacked observations. (b) Sim2real performance showing the percentage of time the pendulum remains upright (within $\pm 10°$ and ± 0.5 rad/s). (c) Performance of a policy using full state estimation with delay compensation, demonstrating the importance of delay compensation for steady performance.

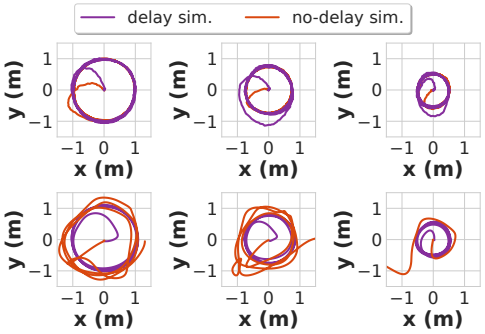

(a) $R = 1.0$m (b) $R = 0.75$m (c) $R = 0.5$m

Figure 9: Sim2real performance of quadrotor policies trained with and without delay simulation across different path radii. Top row: simulated path following at radii $R = 1.0$m, $R = 0.75$m, and $R = 0.5$m. Bottom row: real-world path following shows that delay simulation improves performance and stability, particularly at smaller radii where delays significantly impact control.

4.2 Sim2Real Transfer

To support the claim that our approach implements delay compensation techniques essential for effective sim2real transfer, we evaluate the sim2real performance of policies trained with and without delay compensation for a pendulum and quadrotor systems.

Pendulum Swing-Up This task highlights the challenge of delay compensation and partial observability in reinforcement learning. By demonstrating that neglecting delay simulation can impair policy transfer even in a seemingly simple scenario, we underscore the necessity of delay-aware approaches for more complex systems, where delays are inevitable and system dynamics are more intricate (Liu et al., 2019; Asaamoning et al., 2021; Lou et al., 2019; Peters et al., 2014). The pendulum task's simplicity effectively clarifies the importance of addressing delays in sim2real frameworks.

To investigate the impact of delays and partial observability on task complexity, we train pendulum swing-up policies using PPO (Schulman et al., 2017) under different conditions in simulation. We evaluate policies trained with full state information, stacked observations with and without delay simulation, and estimated full state information with simulated delays. As shown in Fig. 8a, policies with full state information achieve higher rewards and converge faster than those relying on stacked observations, especially when delays are present. This highlights the additional challenge introduced by delays and partial observability, beyond the complexity of the task itself.

Zero-shot evaluations on the real system show that policies trained solely with stacked observations fail to consistently swing up the pendulum, while the policy trained with delay simulation, delay compensation, and full state estimation achieves reliable swing-up, as demonstrated in Fig. 8b. Interestingly, even a policy trained on the full state without simulated delays can achieve consistent swing-up when real-world evaluation uses an estimator that compensates for delays and estimates the full state, as indicated by *pred.* in Fig. 8c.

We assess the performance gains of delay compensation alone versus delay compensation with hidden state estimation, by evaluating the full state policy in two other scenarios: using the angle encoder, which provides full state information with negligible delay compared to camera images, and using the filtered state estimate from the UKF instead of the forward-predicted state. Both policies perform suboptimally, suggesting that both full state estimation and forward prediction are essential for reliable performance, as shown in Fig. 8c.

Path Following with a Quadrotor We trained a quadrotor to fly a circular path at maximum speed with varying radii to assess the impact of delay simulation on sim2real performance. In simulation, all policies achieved successful path following, with the no-delay policy reaching higher speeds and maintaining lower path errors due to its ability to fly more aggressively in the absence of simulated delays, as detailed in Tab. 2. However, in real-world tests, only the policy trained with delay simulation maintained stable flight; the no-delay policy exhibited oscillations around the target path. The performance gap widened at smaller radii, with the no-delay policy ultimately crashing at a radius of 0.5 m, demonstrating the critical role of delay-aware training for reliable real-world deployment, as shown in Fig. 9.

Radii (m)	Simulation				Real-world			
	v_{path} (m/s)		e_{path} (m)		v_{path} (m/s)		e_{path} (m)	
	delay	no-delay	delay	no-delay	delay	no-delay	delay	no-delay
1.00	1.95	**2.23**	0.03	**0.02**	**2.01**	2.00	**0.06**	0.19
0.75	1.67	**1.92**	0.03	**0.02**	**1.64**	1.42	**0.04**	0.32
0.50	1.39	**1.61**	**0.04**	**0.04**	**1.33**	−0.54	**0.04**	0.92

Table 2: Impact of delays on simulated vs. real-world performance across different path radii. Boldface indicates the best performance in each category.

4.3 Computational Complexity Analysis

To support our claim that the framework enables efficient parallelized simulation on accelerator hardware, we evaluated simulation speeds using the COMPILED runtime on an NVIDIA RTX 3070 Laptop GPU. The data flow was augmented with simulator nodes and subsequently parallelized to simulate delays according to real-world settings.

We measured the computation time for CMA-ES (Hansen, 2006) to converge during system identification for the pendulum and quadrotor tasks. For the pendulum, optimizing 27 parameters with a population size of 200 and a 21-second rollout per fitness evaluation (1,050 steps) led to convergence after 38 generations in 22.07 seconds, achieving 380k steps/s with a compilation time of 19.97 seconds. For the quadrotor, optimizing 8 parameters under similar conditions but with a 15-second rollout (375 steps) resulted in convergence after 31 generations in 5.81 seconds, reaching 400k steps/s with a compilation time of 10.16 seconds. We also evaluated PPO training time using the implementation from (Lu et al., 2022): for the pendulum, training 5 policies in parallel with 64 environments reached 5 million steps in 77.1 seconds (325k steps/s), while for the quadrotor, training with 128 environments for 10 million steps completed in 29.8 seconds (336k steps/s), demonstrating the framework's efficiency in supporting rapid training on real-world tasks.

To isolate simulation speed from training overhead, we performed a parallelized rollout speed analysis (Fig. 10). The results show a linear relationship on a logarithmic scale, indicating that as the number of parallel environments doubles, the simulation speed also roughly doubles. An initial superlinear increase is observed, likely due to constant overheads being amortized over a larger number of parallel environments, resulting in more efficient resource utilization. The speed of simulation in our framework is determined by the computational complexity of each node and the ability to parallelize their interactions. Our framework extends beyond standard simulations by modeling the asynchronous interaction between components, which are inherently challenging to parallelize efficiently (van der Heijden et al., 2024a). By demonstrating fast simulation speeds for the pendulum and quadrotor, we show that our framework does not introduce significant overhead beyond the computations within each node. If the simulation speed were slow, even with the simple dynamics of these systems, it would indicate a substantial fixed overhead from the framework.

To support the claim that our framework meets the latency and performance requirements for real-time online processing in real-world systems, we evaluate the latency of different components during real-world experiments. Our framework records timing information for each node, allowing us to estimate computation and communication delay statistics across both the pendulum and quadrotor systems, as visualized in Fig. 5c and Fig. 7c. The mean and standard deviation of delays for each node's periodic computation are calculated,

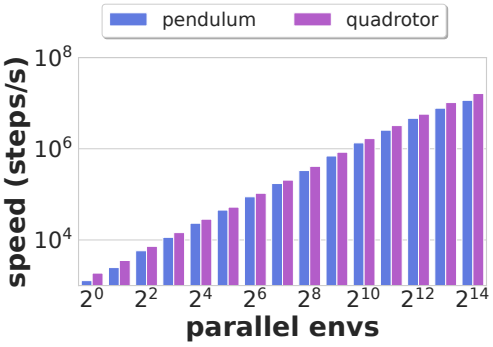

Figure 10: Simulation steps per second vs. number of parallel environments for a 200-step rollout on a GPU. The pendulum (20 ms/step) and quadrotor (25 ms/step) systems both demonstrate a linear scaling in simulation speed with increasing parallel environments.

Node	Delay (ms)	Rate (Hz)	Device	Computation
		Pendulum		
camera	9.8 ± 8.0	60	$\texttt{CPU}_1$	image-to-angle conv.
estimator	3.5 ± 5.2	50	$\texttt{CPU}_2$	UKF update
agent	1.7 ± 2.3	50	GPU	Policy NN(64,64)
motor	5.6 ± 7.0	50	$\texttt{CPU}_3$	Cmd to pendulum
		Quadrotor		
mocap	0.3 ± 0.1	50	$\texttt{CPU}_1$	Read quadrotor pose
agent	2.6 ± 0.5	25	GPU	Policy NN(64,64)
pid	2.8 ± 0.3	50	$\texttt{CPU}_2$	Cmds to quadcopter

Table 3: Delay statistics for Quadrotor and Pendulum nodes, including delay (mean ± std.) in ms, rate in Hz, device type, and a description of each computation. Subscripts indicate dedicated CPU cores. NN denotes a neural network with layer sizes in parentheses.

providing insights into system performance. By dedicating specific CPU cores to each node, we bypass the Python Global Interpreter Lock (GIL), enabling concurrent execution. Additionally, we use the GPU to accelerate policy inference in the agent node. This approach results in low latency across the system. Unexpectedly, the motor node in the pendulum system exhibited large delays, likely due to the hardware's slow response time while servicing ROS (Quigley et al., 2009) service calls. As expected, the camera node had the highest delays, attributed to the time required for image retrieval and processing to convert images to angles.

In summary, our evaluation demonstrates that our approach effectively identifies both dynamics and delays from real-world data, compensates for delays to improve sim2real transfer, and facilitates efficient parallelized simulation on accelerator hardware. At the same time, our approach meets the latency and performance requirements for real-time online processing, supporting all four key claims.

5 Conclusion

In this paper, we presented a novel framework, REX (Robotic Environments with jaX), for sim2real transfer that introduces a graph-based simulation model incorporating latency effects, optimized for parallelization on accelerator hardware. Our approach models asynchronous, hierarchical systems by explicitly representing computation, communication, actuation, and sensing delays. This enables the simultaneous estimation of system dynamics and delays using real-world data, effectively minimizing the sim2real gap. We implemented and evaluated our approach on two real-world robotic systems, demonstrating its ability to support rapid training while maintaining high fidelity to real-world conditions. The experiments suggest that our framework not only improves the accuracy of policy transfer by reducing the impact of delays and partial observability but also enhances simulation efficieny by leveraging hardware acceleration.

For future work, we aim to extend the framework to support estimating stochastic hidden delays, which could further reduce the sim2real gap by more accurately capturing real-world uncertainties. Additionally, we plan to enhance the framework's scalability and real-world applicability by enabling distributed computing across multiple machines, beyond the current capability of utilizing different devices via JAX.

References

Godwin Asaamoning, Paulo Mendes, Denis Rosário, and Eduardo Cerqueira. Drone swarms as networked control systems by integration of networking and computing. *Sensors*, 21(8):2642, 2021.

Frederico Augugliaro, Sergei Lupashin, Michael Hamer, Cason Male, Markus Hehn, Mark W Mueller, Jan Sebastian Willmann, Fabio Gramazio, Matthias Kohler, and Raffaello D'Andrea. The flight assembled architecture installation: Cooperative construction with flying machines. *IEEE Control Systems Magazine*, 34(4):46–64, 2014.

Radhakisan Baheti and Helen Gill. Cyber-physical systems. *The Impact of Control Technology*, 12(1): 161–166, 2011.

Yann Bouteiller, Simon Ramstedt, Giovanni Beltrame, Christopher Pal, and Jonathan Binas. Reinforcement learning with random delays. In *Proc. of the Int. Conf. on Learning Representations (ICLR)*, 2021.

Greg Brockman, Vicki Cheung, Ludwig Pettersson, Jonas Schneider, John Schulman, Jie Tang, and Wojciech Zaremba. OpenAI Gym. *arXiv preprint*, 2016.

Ken Caluwaerts, Atil Iscen, J Chase Kew, Wenhao Yu, Tingnan Zhang, Daniel Freeman, Kuang-Huei Lee, Lisa Lee, Stefano Saliceti, Vincent Zhuang, et al. Barkour: Benchmarking animal-level agility with quadruped robots. *arXiv preprint*, 2023.

Erik Derner, Jiri Kubalik, Nicola Ancona, and Robert Babuska. Constructing parsimonious analytic models for dynamic systems via symbolic regression. *Applied Soft Computing*, 94:106432, 2020.

Norhan Mohsen Elocla, Mohamad Chehadeh, Igor Boiko, Sean Swei, and Yahya Zweiri. The Role of Time Delay in Sim2real Transfer of Reinforcement Learning for Unmanned Aerial Vehicles. In *Proc. of the Int. Conf. on Advanced Robotics (ICAR)*, pp. 514–519. IEEE, 2023.

C Daniel Freeman, Erik Frey, Anton Raichuk, Sertan Girgin, Igor Mordatch, and Olivier Bachem. Brax-A Differentiable Physics Engine for Large Scale Rigid Body Simulation. In *Proc. of the Advances in Neural Information Processing Systems (NeurIPS)*, 2021.

Roy Frostig, Matthew James Johnson, and Chris Leary. Compiling machine learning programs via high-level tracing. *Systems for Machine Learning*, 4(9), 2018.

Nikolaus Hansen. The CMA evolution strategy: a comparing review. *Towards a new evolutionary computation: Advances in the estimation of distribution algorithms*, pp. 75–102, 2006.

Eric Heiden, Christopher E Denniston, David Millard, Fabio Ramos, and Gaurav S Sukhatme. Probabilistic inference of simulation parameters via parallel differentiable simulation. In *Proc. of the IEEE Intl. Conf. on Robotics & Automation (ICRA)*, pp. 3638–3645. IEEE, 2022.

David Hoeller, Nikita Rudin, Dhionis Sako, and Marco Hutter. Anymal parkour: Learning agile navigation for quadrupedal robots. *Science Robotics*, 9(88):eadi7566, 2024.

Yuanming Hu, Luke Anderson, Tzu-Mao Li, Qi Sun, Nathan Carr, Jonathan Ragan-Kelley, and Frédo Durand. DiffTaichi: Differentiable Programming for Physical Simulation. In *Proc. of the Int. Conf. on Learning Representations (ICLR)*, 2020.

Julian Ibarz, Jie Tan, Chelsea Finn, Mrinal Kalakrishnan, Peter Pastor, and Sergey Levine. How to train your robot with deep reinforcement learning: lessons we have learned. *Intl. Journal of Robotics Research (IJRR)*, 40(4-5):698–721, 2021.

Simon J Julier and Jeffrey K Uhlmann. Unscented filtering and nonlinear estimation. *Proceedings of the IEEE*, 92(3):401–422, 2004.

Jacob E Kooi and Robert Babuska. Inclined Quadrotor Landing using Deep Reinforcement Learning. In *Proc. of the IEEE/RSJ Intl. Conf. on Intelligent Robots and Systems (IROS)*, pp. 2361–2368. IEEE, 2021.

Robert Tjarko Lange. evosax: Jax-based evolution strategies. *arXiv preprint*, 2022a.

Robert Tjarko Lange. gymnax: A JAX-based reinforcement learning environment library, 2022b. URL `http://github.com/RobertTLange/gymnax`.

Quentin Le Lidec, Igor Kalevatykh, Ivan Laptev, Cordelia Schmid, and Justin Carpentier. Differentiable simulation for physical system identification. *IEEE Robotics and Automation Letters (RA-L)*, 6(2):3413–3420, 2021.

Xing Liu, Hansong Xu, Weixian Liao, and Wei Yu. Reinforcement learning for cyber-physical systems. In *2019 IEEE International Conference on Industrial Internet (ICII)*, pp. 318–327. IEEE, 2019.

Lennart Ljung. System identification. In *Signal analysis and prediction*, pp. 163–173. Springer, 1998.

Xin Lou, Cuong Tran, David KY Yau, Rui Tan, Hongwei Ng, Tom Zhengjia Fu, and Marianne Winslett. Learning-based time delay attack characterization for cyber-physical systems. In *2019 IEEE International Conference on Communications, Control, and Computing Technologies for Smart Grids (SmartGridComm)*, pp. 1–6. IEEE, 2019.

Chris Lu, Jakub Kuba, Alistair Letcher, Luke Metz, Christian Schroeder de Witt, and Jakob Foerster. Discovered policy optimisation. *Proc. of the Advances in Neural Information Processing Systems (NeurIPS)*, 35:16455–16468, 2022.

Mayank Mittal, Calvin Yu, Qinxi Yu, Jingzhou Liu, Nikita Rudin, David Hoeller, Jia Lin Yuan, Ritvik Singh, Yunrong Guo, Hammad Mazhar, Ajay Mandlekar, Buck Babich, Gavriel State, Marco Hutter, and Animesh Garg. Orbit: A Unified Simulation Framework for Interactive Robot Learning Environments. *IEEE Robotics and Automation Letters (RA-L)*, pp. 1–8, 2023. doi: 10.1109/LRA.2023.3270034.

Oliver Nelles. *Nonlinear dynamic system identification.* Springer, 2020.

NVIDIA. NVIDIA PhysX, 2020. URL `\url{https://developer.nvidia.com/physx-sdk}`.

Andrés A Peters, Richard H Middleton, and Oliver Mason. Leader tracking in homogeneous vehicle platoons with broadcast delays. *Automatica*, 50(1):64–74, 2014.

Morgan Quigley, Ken Conley, Brian Gerkey, Josh Faust, Tully Foote, Jeremy Leibs, Rob Wheeler, Andrew Y Ng, et al. ROS: an open-source Robot Operating System. *Proc. of the IEEE Intl. Conf. on Robotics & Automation (ICRA)*, 3:5, 2009.

Nikita Rudin, David Hoeller, Philipp Reist, and Marco Hutter. Learning to Walk in Minutes Using Massively Parallel Deep Reinforcement Learning. *Proc. of the Conf. Robot Learning (CoRL)*, 164:91–100, 2022.

Erik Schuitema, Lucian Busoniu, Robert Babuska, and Pieter Jonker. Control delay in reinforcement learning for real-time dynamic systems: A memoryless approach. In *Proc. of the IEEE/RSJ Intl. Conf. on Intelligent Robots and Systems (IROS)*, pp. 3226–3231. IEEE, 2010.

John Schulman, Filip Wolski, Prafulla Dhariwal, Alec Radford, and Oleg Klimov. Proximal policy optimization algorithms. *arXiv preprint*, 2017.

Michael Sherback, Oliver Purwin, and Raffaello D'Andrea. Real-time motion planning and control in the 2005 cornell robocup system. In *Robot Motion and Control: Recent Developments*, pp. 245–263. Springer, 2006.

Naoki Shibata. Efficient Evaluation Methods of Elementary Functions Suitable for SIMD Computation. *Computer science-Research and development*, 25:25–32, 2010.

Otto JM Smith. Closer control of loops with dead time. *Chemical engineering progress*, 53:217–219, 1957.

Jie Tan, Tingnan Zhang, Erwin Coumans, Atil Iscen, Yunfei Bai, Danijar Hafner, Steven Bohez, and Vincent Vanhoucke. Sim-to-real: Learning agile locomotion for quadruped robots. *arXiv preprint*, 2018.

Yujin Tang, Yingtao Tian, and David Ha. EvoJAX: Hardware-Accelerated Neuroevolution. *arXiv preprint*, 2022.

Russ Tedrake and the Drake Development Team. Drake: Model-based design and verification for robotics. `https://drake.mit.edu`, 2019.

Emanuel Todorov, Tom Erez, and Yuval Tassa. MuJoCo: A physics engine for model-based control. *Proc. of the IEEE/RSJ Intl. Conf. on Intelligent Robots and Systems (IROS)*, pp. 5026–5033, 2012.

Heinz Unbehauen and GP Rao. Continuous-time approaches to system identification—a survey. *Automatica*, 26(1):23–35, 1990.

Bas van der Heijden, Laura Ferranti, Jens Kober, and Robert Babuska. Efficient Parallelized Simulation of Cyber-Physical Systems. *Trans. on Machine Learning Research (TMLR)*, 2024a. ISSN 2835-8856. URL `https://openreview.net/forum?id=VzKXbCzNoU`. Reproducibility Certification.

Bas van der Heijden, Jelle Luijkx, Laura Ferranti, Jens Kober, and Robert Babuska. Engine Agnostic Graph Environments for Robotics (EAGERx): A Graph-Based Framework for Sim2real Robot Learning. *IEEE Robotics and Automation Magazine (RAM)*, pp. 2–15, 2024b. doi: 10.1109/MRA.2024.3433172.

Peter Van Overschee and BL0888 De Moor. *Subspace identification for linear systems: Theory—Implementation—Applications*. Springer Science & Business Media, 2012.

Yuxiang Yang, Ken Caluwaerts, Atil Iscen, Tingnan Zhang, Jie Tan, and Vikas Sindhwani. Data efficient reinforcement learning for legged robots. *Proc. of the Conf. Robot Learning (CoRL)*, pp. 1–10, 2020.